

## **Supplementary Information (PDF)**

### ***A screening based approach to circumvent tumor microenvironment-driven intrinsic resistance to BCR-ABL+ inhibitors in Ph+ acute lymphoblastic leukemia***

Harpreet Singh<sup>1†</sup>, Anang A. Shelat<sup>2</sup>, Amandeep Singh<sup>3</sup>, Nidal Boulos<sup>1</sup>, Richard T. Williams<sup>1‡</sup>, R. Kiplin Guy<sup>2‡\*</sup>

<sup>1</sup>Department of Oncology,

<sup>2</sup>Department of Chemical Biology and Therapeutics,

St. Jude Children's Research Hospital, 262 Danny Thomas Place, Memphis, TN, 38105

<sup>3</sup>Department of Medicine,

Kings County Hospital Center, 451 Clarkson Avenue, Brooklyn, NY, 11203

<sup>†</sup>Integrated Program in Biomedical Sciences,

University of Tennessee Health Science Center, 920 Madison, Memphis, TN, 38103

<sup>‡</sup>Current address: Puma Biotechnology Inc., Los Angeles, CA 90024

\* For Correspondence:

Kip Guy, Ph.D

Department of Chemical Biology and Therapeutics, St. Jude Children's Research Hospital,  
Memphis, TN 38105-3678. Tel: 901-595-5714, Fax: 901-595-2715, Email: [kip.guy@stjude.org](mailto:kip.guy@stjude.org)

This Supplementary Information (PDF) section comprises of table of contents; materials and methods for FACS assessment of viability; FACS assessment of cell cycle percentages; drug/cytokine washout and cytokine recovery studies; dasatinib re-challenge studies; detailed description of chemical library screened; HT drug screens - data processing, quality control and hit scoring criteria; cluster analysis of hits using therapeutic drug classes; Supplementary Figures S1-S11 with legends; Supplementary Table 1 and Supplementary References.

**Table of contents for Supplementary Information (PDF):**

<b>Production and culture of murine leukemia initiating cells (LICs) .....</b>	<b>3</b>
<b><i>In vivo</i> adoptive leukemia transfer Ph+ ALL model .....</b>	<b>3</b>
<b>FACS assessment of viability .....</b>	<b>4</b>
<b>FACS assessment of cell cycle percentages.....</b>	<b>4</b>
<b>Detailed description of chemical library screened.....</b>	<b>6</b>
<b>Data processing, quality control and hit scoring criteria for HT drug screens .....</b>	<b>7</b>
<b><i>In vivo</i> preclinical therapeutic studies.....</b>	<b>10</b>
<b>Bioluminescent imaging and evaluation of cures.....</b>	<b>10</b>
<b>Supplementary Figure S1: .....</b>	<b>11</b>
<b>Supplementary Figure S2: .....</b>	<b>12</b>
<b>Supplementary Figure S3: .....</b>	<b>13</b>
<b>Supplementary Figure 4:.....</b>	<b>14</b>
<b>Supplementary Figure 5:.....</b>	<b>15</b>
<b>Supplementary Figure 6:.....</b>	<b>16</b>
<b>Supplementary Figure S9: .....</b>	<b>20</b>
<b>Supplementary Figure S10: .....</b>	<b>21</b>
<b>Supplementary Figure S11: .....</b>	<b>22</b>
<b>Supplementary Table 1: .....</b>	<b>23</b>
<b>Supplementary References.....</b>	<b>25</b>

## **Production and culture of murine leukemia initiating cells (LICs)**

Replication-defective mouse stem cell virus (MSCV) retroviral vectors co-expressing either the wild-type (WT) allele of human p185<sup>BCR-ABL</sup> or mutant BCR-ABL alleles p185<sup>T315I</sup> or p185<sup>F317L</sup>, and either green fluorescent protein (GFP) or luciferase, were packaged into replication-incompetent ecotropic virions[17,18,22]. Whole bone marrow cell suspensions from *Arf*<sup>-/-</sup> young adult mice were transduced to produce *Arf*<sup>-/-</sup> p185+ pre-B LICs [17,22]. After initial establishment on autologous stromal cell layers over 7 days, transformed pre-B cells were briefly expanded in the absence of a stromal layer for 2 days in liquid culture in BCM10 media (RPMI1640 supplemented with 10% Hyclone fetal calf serum, 4 mM glutamine, 100 Units/mL penicillin, 100 µg/mL streptomycin, and 55 µM beta-mercaptoethanol[18]), and cryopreserved. Prior to use in any assays, *Arf*<sup>-/-</sup> p185<sup>WT</sup> and *Arf*<sup>-/-</sup> p185<sup>T315I</sup> pre-B cells (BCR-ABL<sup>WT</sup> LICs and BCR-ABL<sup>T315I</sup> LICs, respectively) were thawed and allowed to recover and expand exponentially in BCM10 for 3 days.

## ***In vivo* adoptive leukemia transfer Ph+ ALL model**

Mice were housed in an American Association of Laboratory Animal Care (AALAC)– accredited facility and treated on Institutional Animal Care and Use Committee (IACUC)– approved protocols in accordance with NIH guidelines. Adoptive cell transfers were performed by injecting LICs into tail veins of healthy, non-conditioned, immune-competent 10- to 12-week-old IL-7<sup>+/+</sup> or IL-7<sup>-/-</sup> C57Bl/6J mice (Jackson Labs, Bar Harbor, ME). Animals were observed daily and sacrificed when moribund (dehydration, ruffled fur, poor mobility, respiratory distress). Survival curves were generated using GraphPad Prism Version 5.0 (La Jolla, CA). The Mantel-Cox test was applied to pairwise comparisons of survival data.

### **FACS assessment of viability**

Viability of LICs was estimated after counterstaining approximately  $5 \times 10^5$  LICs (in 0.5 mL volume) with 35  $\mu$ L of a propidium iodide (PI) solution (0.25 mg/mL in PBS). The percentage of viable cells was calculated by electronic gating on PI-negative cells on PI versus forward scatter dot plots, with forward scatter signals consistent with LICs, and comparison of this number with total cell number. Data were collected and analyzed on a BD Biosciences LSR II flow cytometer (San Jose, CA), using BD Biosciences FACS DiVa software.

### **FACS assessment of cell cycle percentages**

For determination of percentages in cell cycle phases,  $5 \times 10^5$  LICs were centrifuged, washed once with PBS, re-centrifuged, and cell pellets were resuspended in 0.5 mL PI staining solution (0.05 mg/mL PI, 0.1% sodium citrate, 0.1% Triton X100), which lysed the cells and stained nuclear DNA with PI. Samples were then treated with DNase-free RNase (0.2 mg/mL in 10 M Tris-HCl/15 mM NaCl, pH 7.5) for 30 min at room temperature, filtered, and analyzed for red fluorescence from a PI-labeled DNA on BD Biosciences FACS Calibur flow cytometer (San Jose, CA) by using BD Biosciences CellQuest Pro software. The percentages of cells within each cell cycle phase were computed using the computer program ModFit (Verity Software House, Topsham, ME).

**Drug/cytokine washout and cytokine recovery studies**

For washout studies, BCR-ABL<sup>WT</sup> LICs were diluted to a density of  $1 \times 10^5$  LICs/mL in BCM-10 containing no or 5 mg/mL IL7, and treatment with either dasatinib or 0.1% DMSO by volume (non-drug treated controls) was initiated at time 0 h in triplicate 100 mm petri dishes. Daily monitoring for expected drug-induced changes was performed by naked-eye microscopy from 0 to 72 h. At the 72 h time point, after harvesting under identical conditions, total LIC density and viability percentage for all samples were determined using Beckman Coulter Vi-cell (trypan

blue) in triplicates. Each sample was spun down in 50 mL BD Falcon™ tubes; the supernatant was discarded and LIC pellet resuspended in freshly prepared BCM-10 (not containing any cytokine or drug). This washing step was repeated 4 times to ensure complete removal of the drug and/or cytokine. After the last wash, each pellet was resuspended to  $1 \times 10^6$  total LICs per mL master stocks. Aliquots from master stocks were taken for (i) flow assessment of viability and cell cycle percentages (as described above); (ii) manual CTG assay using 25 uL sample per well in 384-well microplates (in triplicates), as an independent determination for LIC growth. For assessment of extracellular cytokine on recovery of LICs that were previously challenged with dasatinib (0 to 72 h), washed master stocks were diluted to  $5 \times 10^5$  total LICs per mL in BCM10 with or without 5 ng/mL IL7, plated in 6 well plates (10 cm<sup>2</sup> approx), and incubated at 37°C from 72 to 144 h for recovery, during which time daily naked-eye microscopic examinations were performed. At 144 h, for each sample total LIC density and viability percentage assessment by Beckman, viability and cell cycle percentages by flow assessment and independent CTG evaluations were performed as described for the 72 h time point. Cell growth trends by CTG readout corroborated the findings from trypan blue (Beckman) and DAPI staining (FACS). Key results are presented in **Supplementary Figure S6**; total viable LICs in a sample were calculated as a product of absolute LIC count determined by Beckman and absolute sample viability determined by FACS analysis. **Dasatinib re-challenge studies**

Further studies were performed to evaluate the possibility of a genetically drug-resistant subpopulation that could undergo selection with dasatinib/IL7 co-treatment during 0-72 h of dasatinib/cytokine washout studies above. To this aim, BCR-ABL<sup>WT</sup> LICs were treated with 100 nM dasatinib or 0.1% DMSO in the absence or presence of 5 ng/mL IL7 in 100 mm dishes from 0-72 h, as described above; in addition, a dasatinib challenge (first-time challenge) across 6 log-

fold concentration in the presence or absence of 5 ng/mL IL7 was also performed using CTG assay during this time period (0-72 h). At 72 h, dasatinib/IL7 co-treated LICs from 100 mm dishes were washed (as described above) and immediately challenged (second challenge) from 72 to 144 h with six log-fold concentration range of dasatinib in 384-well microplates either in the presence or absence of 5 ng/mL IL7 using CTG assay. At 144 hrs, dasatinib showed similar potency against LICs in the absence of IL7, irrespective of previous dasatinib exposure. Furthermore, potency of dasatinib was blunted, to a similar extent, during both the first and second drug challenges only when extracellular IL7 was present (data not shown).

### **Detailed description of chemical library screened**

The screening library consisted of 5600 (approximately 3200 unique) approved drugs and chemicals with known biological activity (bioactives). The library was assembled from 3 commercial suppliers: Microsource, Prestwick, and Sigma. The Microsource compounds included the following: (a) the Spectrum collection, which contains 2000 biologically active and structurally diverse compounds, including known drugs, experimental bioactives, and pure natural products(1, 2); (b) the US Drug Collection, which contains 1040 drugs that have reached clinical trials in the US and have been assigned USAN or US Pharmacopeia status; and (c) the Killer collection, which contains a reference set of 160 synthetic and natural toxic substances (<http://www.msdiscovery.com/index.html>). The Prestwick compounds include 1120 small molecules selected for high chemical and pharmacologic diversity. Ninety percent of the collection is composed of known marketed drugs, and the remainder includes bioactive alkaloids or related substances. Human bioavailability and human toxicity data are available for most compounds (<http://www.prestwickchemical.fr/index.php?pa=26>). The Sigma LOPAC1280 (Library of Pharmacologically Active Compounds) collection reflects the most commonly

screened targets in the drug discovery community, including marketed drugs, failed development candidates, and "gold standards" that have well-characterized activities (<http://www.sigmaaldrich.com/chemistry/drug-discovery/validation-libraries.html>).

### **Data processing, quality control and hit scoring criteria for HT drug screens**

All data processing and visualization was performed using custom programs written in the Pipeline Pilot platform (Accelrys, v.7.5) and the R program 6.6(3, 4). The R drc package was used to fit sigmoidal curves(4). ROC statistics were computed using the ROCR package(5).

The quality of the primary drug-screening studies, performed in parallel against BCR-ABL<sup>WT</sup> and BCR-ABL<sup>T315I</sup> LICs, was evaluated by multiple methods including, but not limited to, identification of known antileukemic agents, identification of multiple compound replicates intentionally included in the 5600 collection, and Z' and other screening quality metrics (described in **Supplementary Figures S7 to S10**). In the screening experiments, all assay plates demonstrated attenuation of dasatinib potency in presence of IL7 or BCR-ABL mutation, similar to results described in **Figure 1a and 1b**. An empirically determined, statistically significant but liberal cut-off of >10% activity was chosen to include agents of relatively lower activity considering the high-risk nature of Ph+ ALL and the drug-rich nature of the library as well as to allow for a more complete structure-activity relationship and therapeutic class analysis after subsequent potency determination through secondary screening

The discriminatory power of the phenotypic assay was assessed using receiver operating characteristic (ROC) statistics. A total of 165 compounds were selected to sample the primary assay according to the distribution of observed activities. ROC curves are shown in **Supplementary Figure S10**. The assay has good discriminatory power; with similar AUCs of

approximately 0.83 and 0.85 against BCR-ABL<sup>WT</sup> and BCR-ABL<sup>T315I</sup> LICs, respectively (an ideal assay has an AUC of 1.0, whereas a random assay has an AUC of 0.5).

The activity class designations in the **Excel Supplement** were assigned based on the curve score and visual inspection of dose-response curves. The curve score is a 4 character code derived from the following heuristic:

- First character: letter (A,B,C or D) indicating curve quality
  - D = less than 2 points above the noise (defined as outliers from the negative control population)
  - C =  $r^2 < 0.50$  or range  $> 200\%$  or EC<sub>50</sub>  $>$  maximum concentration tested
  - A =  $r^2 > 0.80$  and difference between two last points  $< 10\%$  (indicating saturation)
  - B = not A,C, or D
  - N prefix = activity decreases with increase concentration
- Second character: number (1-6) indicating potency
  - 1 = EC<sub>50</sub>  $< 0.1 \mu M$
  - 2 =  $0.1 \mu M \geq EC_{50} < 1.0 \mu M$
  - 3 =  $1.0 \mu M \geq EC_{50} < 10.0 \mu M$
  - 4 = EC<sub>50</sub>  $> 10.0 \mu M$
  - 5 = all C and D curves are assigned 5
- Third character: number (1-6) indicating efficacy
  - 1 =  $75\% \geq range < 200\%$
  - 2 =  $50\% \geq range < 75\%$
  - 3 =  $25\% \geq range < 50\%$
  - 4 = range  $< 25\%$

- 5 = all C and D curves are assigned 5
- Fourth character: number (1-6) indicating hill slope
  - 1 = hill  $\leq$  2
  - 2 = 2 < hill  $\leq$  4
  - 3 = 4 < hill  $\leq$  8
  - 4 = hill > 8
  - 5 = all C and D curves are assigned 5

A complete list of all compounds evaluated in the secondary drug-screening experiments with their structure, supplier information, synonyms, EC<sub>50</sub> values, and therapeutic classification is reported in the **Excel Supplement.Cluster analysis of hits using therapeutic classes**

The therapeutic cluster graph was generated by first assigning each compound an Anatomical Therapeutic Chemical Classification System (ATC). This classification system groups drugs into a 5 level hierarchy according to therapeutic indication and chemical properties. The first level indicates anatomical main group and consists of 1 letter; the second level indicates therapeutic main group and consists of 2 digits; the third level indicates therapeutic or pharmacological subgroup and consists of 1 letter; the fourth level indicates chemical, therapeutic or pharmacological subgroup and consists of one letter; and the fifth level indicates the chemical substance and consists of 2 digits. The resulting 7 characters constitute an ATC code, and a compound can be assigned multiple ATC codes. ATC codes can be depicted as a network graph by defining a node to represent each level in the ATC code and then connecting nodes according to parent-child relationships (e.g., first-level node A is the parent of second level nodes A01, A02, etc.). Compounds without an ATC code were assigned based on similarity to known agents, or were assigned to custom codes located under the parent V99

(labeled as “Not defined in ATC” in Figure 2). See Supplementary Figure 10 for the frequency of ATC Level 1 and Level 2 codes among the 706 compounds submitted to dose-response analysis.

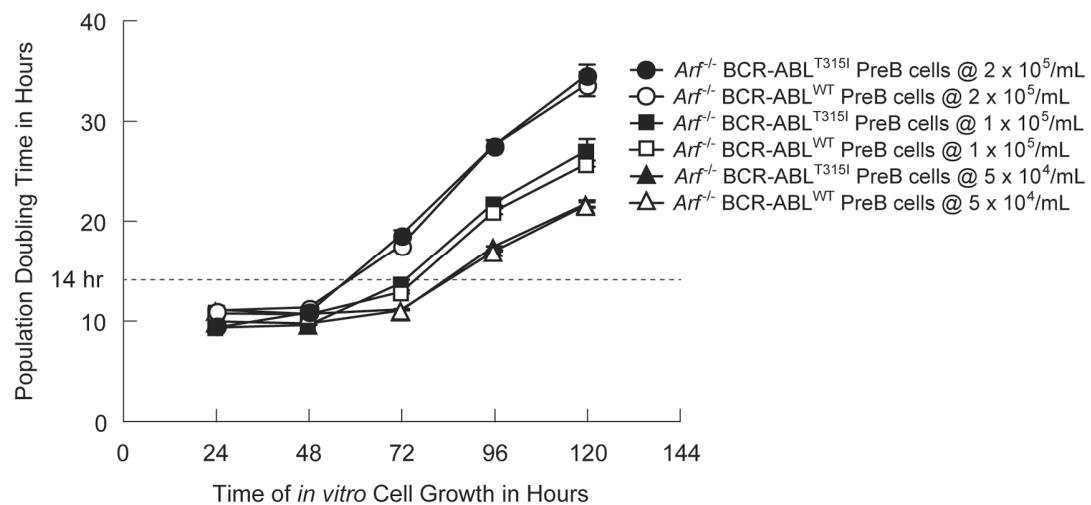
The resulting network was visualized in Cytoscape (v 2.8.1) using the yFiles circular layout algorithm(6). The cytoscape file for this network is available for download as part of this supplement.

### ***In vivo* preclinical therapeutic studies**

For *in vivo* use, dasatinib (LC Labs, Woburn, MA) in citric acid (pH 3.1) [25], and DHA (Avachem, San Antonio, TX) in 0.5% carboxy-methylcellulose/0.5% Tween 80/0.5% benzyl alcohol, were administered by oral gavage. In toxicity studies (data not shown), DHA was ranged up to 300 mg/kg as a single or split dose for 5 days/week over a six week time period. Repeated single doses of 300 mg/kg (5 days/week) were determined to induce no significant weight loss, lethargy, seizures or deaths [26]. During therapeutic studies, animal weights were monitored daily to ensure no significant body weight reductions.

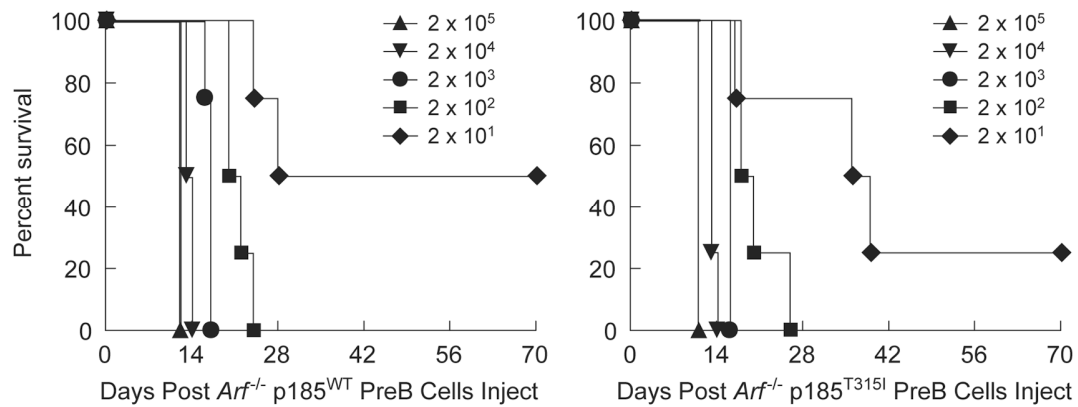
### **Bioluminescent imaging and evaluation of cures**

Bioluminescent imaging and analysis were performed using a Xenogen IVIS-200 system and Living Image software 3.01 (Caliper Life Sciences, Hopkinton, MA)[17]. Total bioluminescent flux measurements (photons/second) were quantified over the whole animal body. Recipient mice that remained clinically healthy 12 months after terminating therapy and had no detectable bioluminescent signal *in vivo* were designated “long-term survivors.”

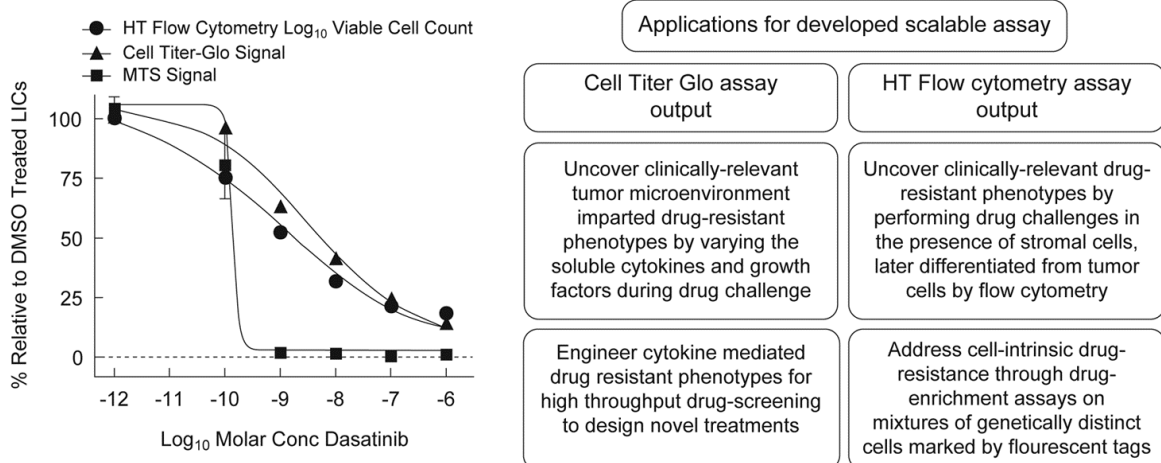


**Supplementary Figure S1: Comparison of the growth properties of  $\text{Arf}^{-/-} \text{p185}^{\text{WT}}$  (filled symbols) and  $\text{Arf}^{-/-} \text{p185}^{\text{T315I}}$  preB (empty symbols) populations during *in vitro* cell culture.**

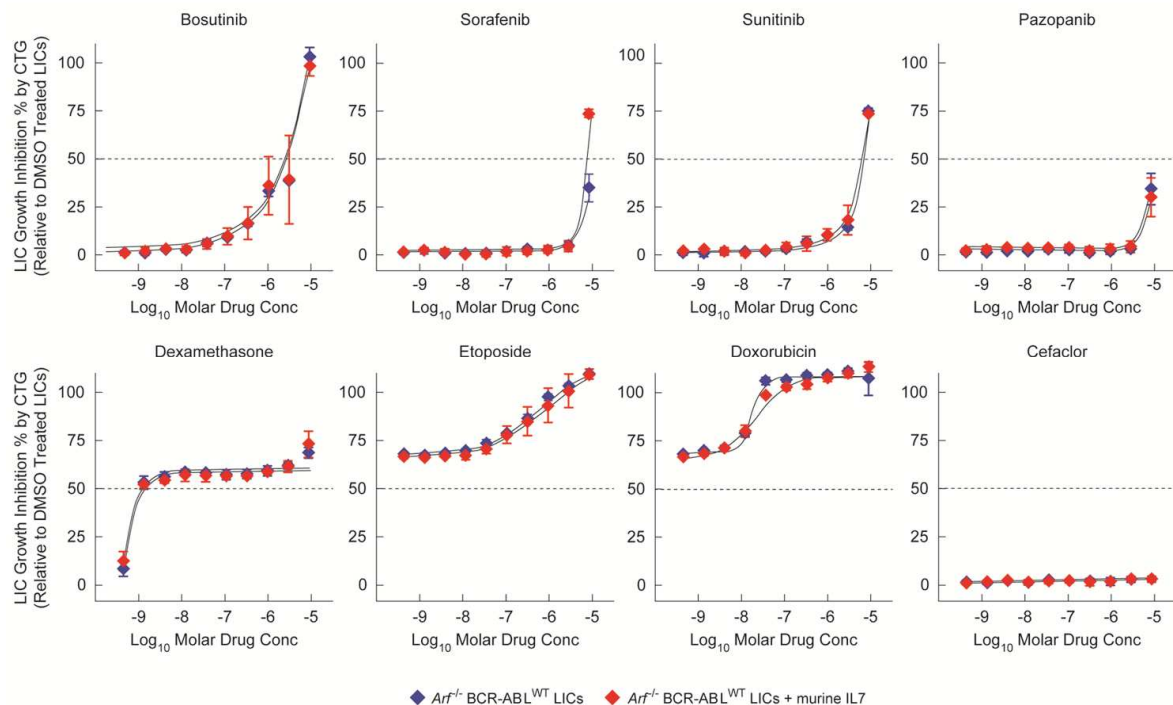
Both cell types were plated at multiple cell dilutions ( $n=3$  for each condition, time=0 h) in 6-well plates and serially followed daily for 5 days to evaluate absolute viable cell count, total viability, doubling times, and total population doublings, using the Beckman Coulter cell counter (trypan blue staining) and fluorescence-activated cell sorting (FACS) analysis in parallel. Both cell types had identical growth properties. Only the comparison for population doubling time in hours (+/- sd) for 3 relevant plating densities is presented. FACS cell-cycle analysis confirmed that a population doubling time less than 14 h was sufficient to maintain cells in exponential growth (>50% cells in S-phase).



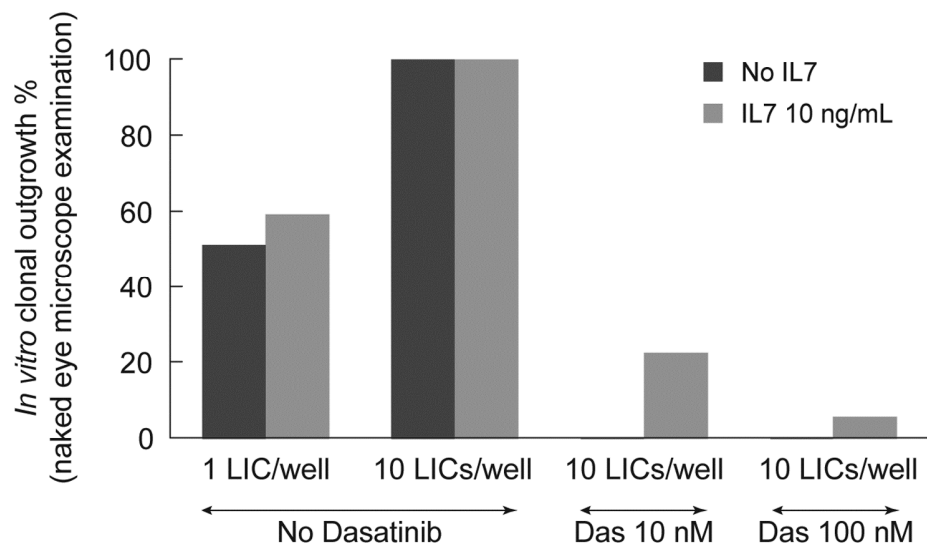
**Supplementary Figure S2: Leukemia stem cell function (LSC) function assay by serial dilution and implantation comparing the *in vivo* leukemia initiating capacity of  $\text{Arf}^{-/-}$  p185<sup>WT</sup> (left) and  $\text{Arf}^{-/-}$  p185<sup>T315I</sup> preB (right) populations. Kaplan-Meier curves represent the overall survival of nonconditioned immunocompetent C57Bl/6J recipient mice that received serial log-fold dilutions (n=4 per arm) of LIC-number (as indicated in the inset legend) on day 0.  $\text{Arf}^{-/-}$  p185-transformed preB murine cells are hereafter referred as LICs.**



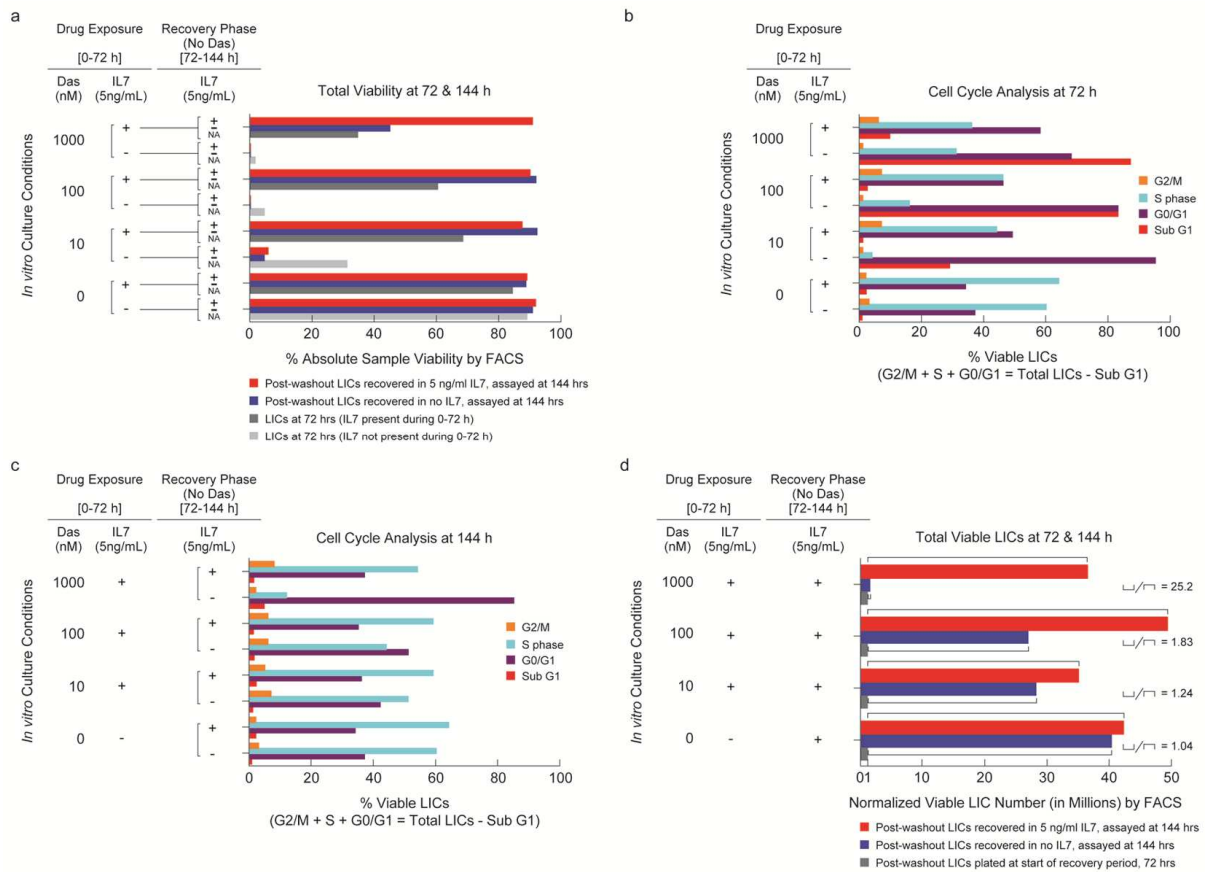
**Supplementary Figure S3: Optimization of the high-throughput LIC-based phenotypic assay.** *BCR-ABL<sup>WT</sup> LICs plated at  $5 \times 10^4$  per mL were challenged with 6 log-fold concentration range of dasatinib or DMSO in 384-well microplates. After a 72 h drug challenge, LIC growth was measured by 3 cellular readouts: CellTiter-Glo (CTG) assay (ATP content), MTS assay (viability), and high-throughput flow cytometry (total viability and viable cell counts by DAPI exclusion). Measured assay readouts at various drug concentrations (x-axis) were normalized to DMSO-treated LICs and graphed (+/- sd) on y-axis. Total viable LIC counts were determined by FACS, reflecting dasatinib-induced phenotypic changes across a 6 log-fold drug-concentration, were closely paralleled by the CTG cellular assay output but not by the commonly used MTS assay.*



**Supplementary Figure 4: Comparative evaluation of IL7-mediated protection conferred against non-BCR-ABL-specific targeting drugs (top panel) and conventional cytotoxic antileukemic clinical drugs (bottom panel).** BCR-ABL<sup>WT</sup> LICs were treated with indicated drugs or DMSO (no drug) for 72 h in the absence (blue) or presence (red) of high (10 ng/mL) murine IL7, in triplicates. The antibiotic drug Cefaclor (often used in leukemia clinics) was used as a non-antileukemic drug control. For each drug concentration, LIC growth was measured by the CTG assay and average values were normalized to DMSO-treated LICs and graphed (+/- sd).

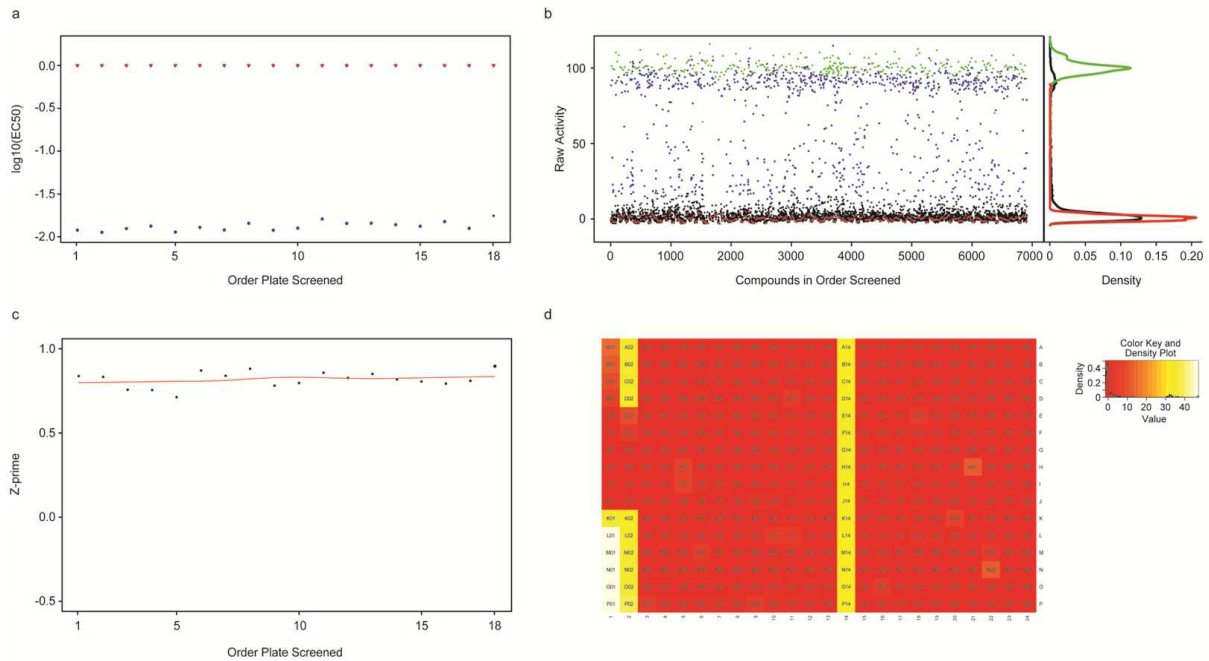


**Supplementary Figure 5: *In vitro* leukemia clonal outgrowth efficiency assays.** Either 1 or 10 viable BCR-ABL<sup>WT</sup> LICs per well sorted by single-cell flow cytometry into 3 clear-bottom 384-well plates for each condition ( $n=1152$ ) were treated ( $t=0$ ) with DMSO (0.1 % by volume) or dasatinib in the absence (black) or presence (grey) of IL7 (10 ng/mL). After 8 days of incubation, naked-eye microscopic examination was performed. Wells showing significant positive growth (approximately  $\geq 50$  LICs per well) were scored positive and percentage of positive wells for each condition indicated on the x-axis was calculated.

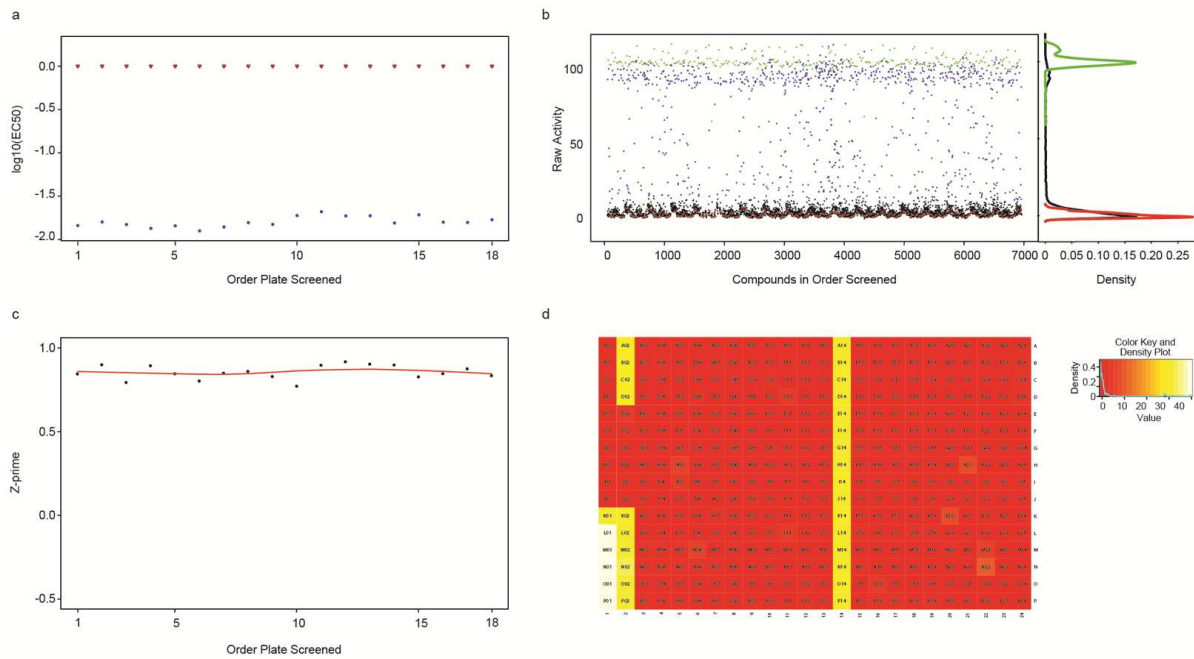


**Supplementary Figure 6: Protection of BCR-ABL<sup>WT</sup> LICs by IL7 during dasatinib exposures (0 to 72 h) and in the post-exposure recovery period (72 to 144 h, no dasatinib). See Supplementary Methods above for details.** (a) Total sample viabilities (DAPI staining, FACS) at the end of exposure period (dark gray=IL7; light gray=No IL7) and recovery period (red=IL7; blue=No IL7). Light gray vs. dark gray comparison depicts significant IL7 protection during dasatinib exposures. Few LICs surviving dasatinib exposures in the absence of IL7 (light gray), later deteriorated and died during recovery period, irrespective of IL7, confirming that BCR-ABL inhibitor exposures commit BCR-ABL+ cells to death(7). IL7 significantly improved recovery of dasatinib/IL7 co-treated LICs (red vs blue), clearly evident at 1000 nM but not at 100 nM and 10 nM dasatinib concentration because of over-confluent growth in presence of IL7.

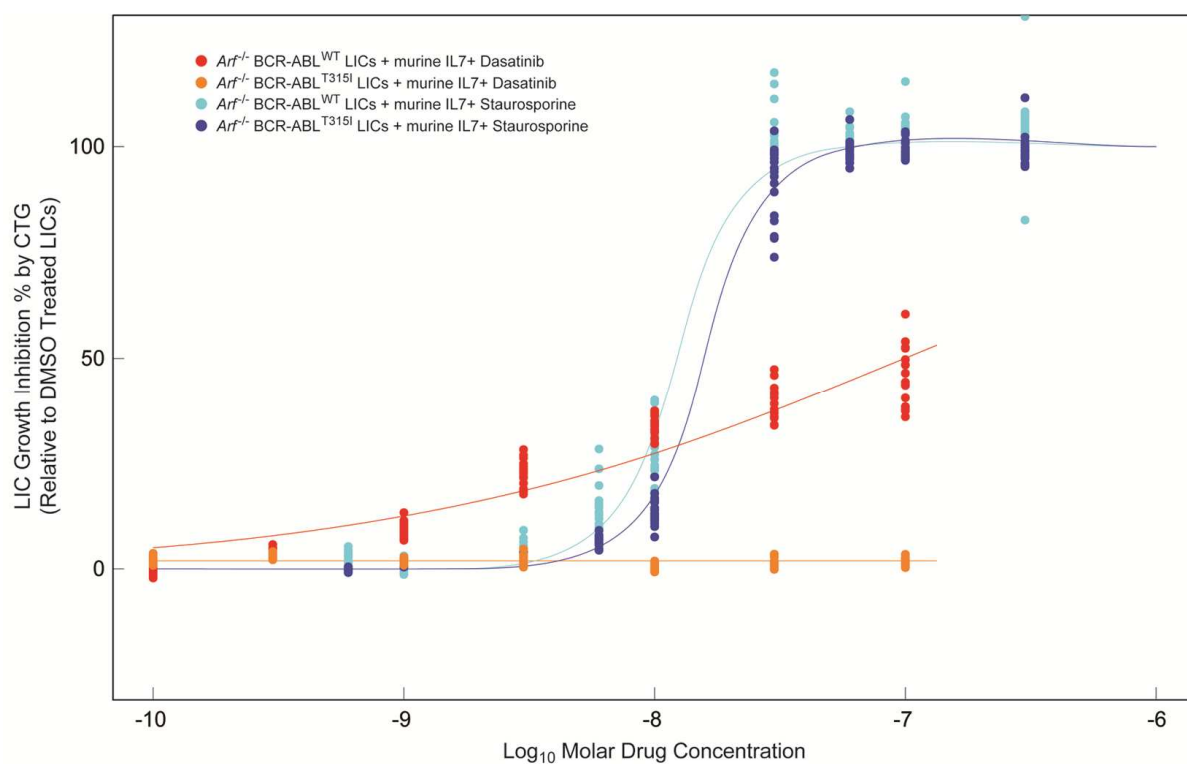
(see Methods, (c) and (d)). **(b)** Cell cycle changes (FACS) at the end of exposure period (corresponding to light and gray bars in (a)). Incremental dasatinib doses (which cause incremental BCR-ABL inhibition(8)) induced cell cycle arrest and apoptosis; IL7 significantly protected LICs from these changes **(c)** Cell cycle analysis at the end of recovery period (corresponding to blue and red in (a)). **(d)** Conditions showing positive LIC growth during recovery period, normalized for equal number of LICs plated at start of recovery (dark grey). Ratio of fold LIC-change in presence (face-down bracket) to that in absence (face-up bracket) of IL7 increased in LICs with higher previous BCR-ABL inhibition from higher dasatinib concentrations during exposure period.



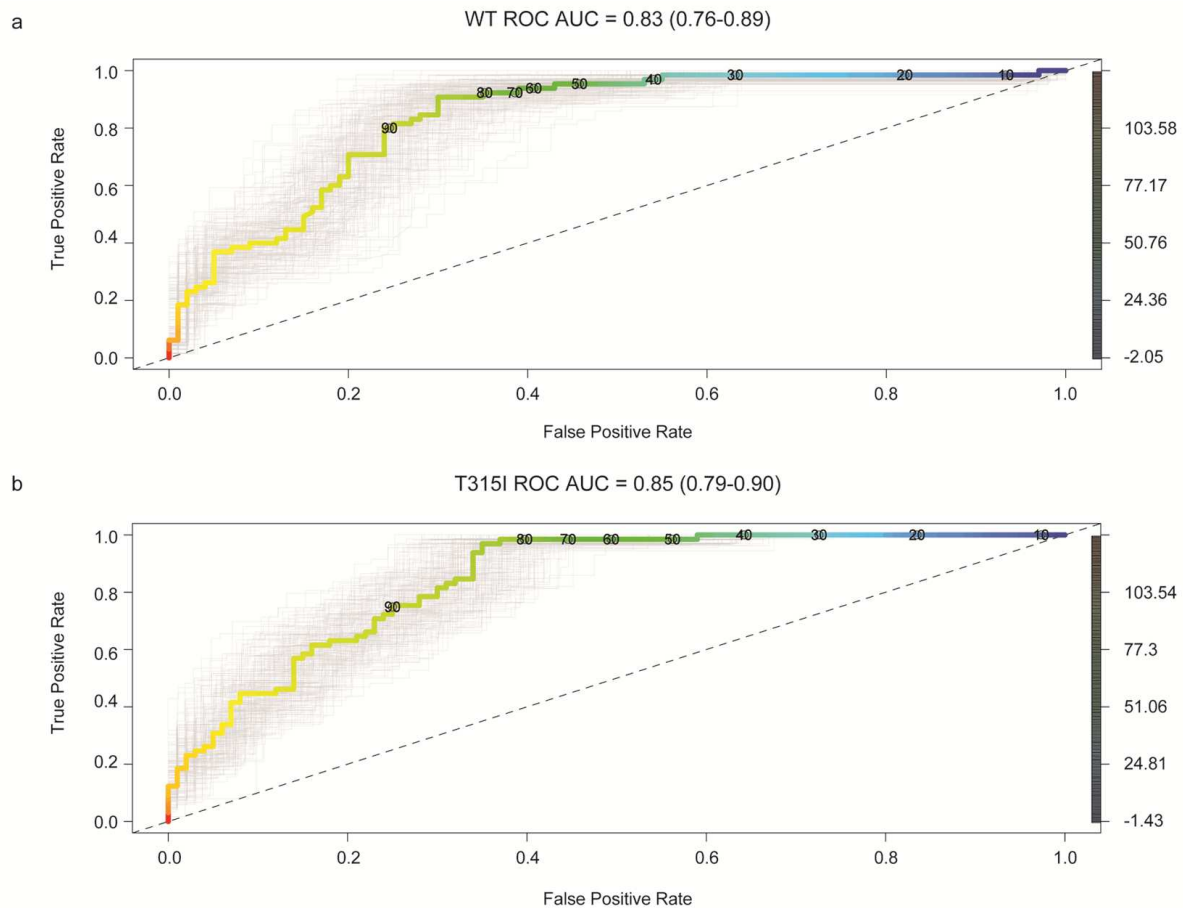
**Supplementary Figure S7: Quality control for the primary screen of 5600 agents against  $\text{BCR-ABL}^{\text{WT}}$  LICs performed in the presence of 0.85 ng/mL IL7. See Supplementary table 1 for well locations.** (a) Distribution of  $\text{EC}_{50}$  of non- $\text{BCR-ABL}$ -inhibiting reference compound staurosporine (calculated from wells 2A-2J in (d)). (b) Scatter plot of percent activity of the test compounds relative to controls. Good separation is seen between negative controls (red, DMSO-treated. max signal, column 13 in (d)) and positive controls (green, 300 nM staurosporine, min signal, column 14 in (d)). Test compounds showing statistically significant activity relative to background noise (negative controls, red) are depicted in blue and inactive test compounds in black. Densities for positive, negative, and test compounds are shown on the right. (c) Distribution of Z' values for each plate in the primary screen. All Z' values throughout the run – average=0.82, lowest=0.71 and highest=0.9 (d) Heat map comparison of well activity averaged across all plates. Wells 1A-1J and 2A-2J show serial dilutions of dasatinib and staurosporine. In presence of IL7, average LIC growth inhibition of approx. 45% was achieved by 100 nM dasatinib (well 1A), the later approaching maximum concentration achieved in human plasma.



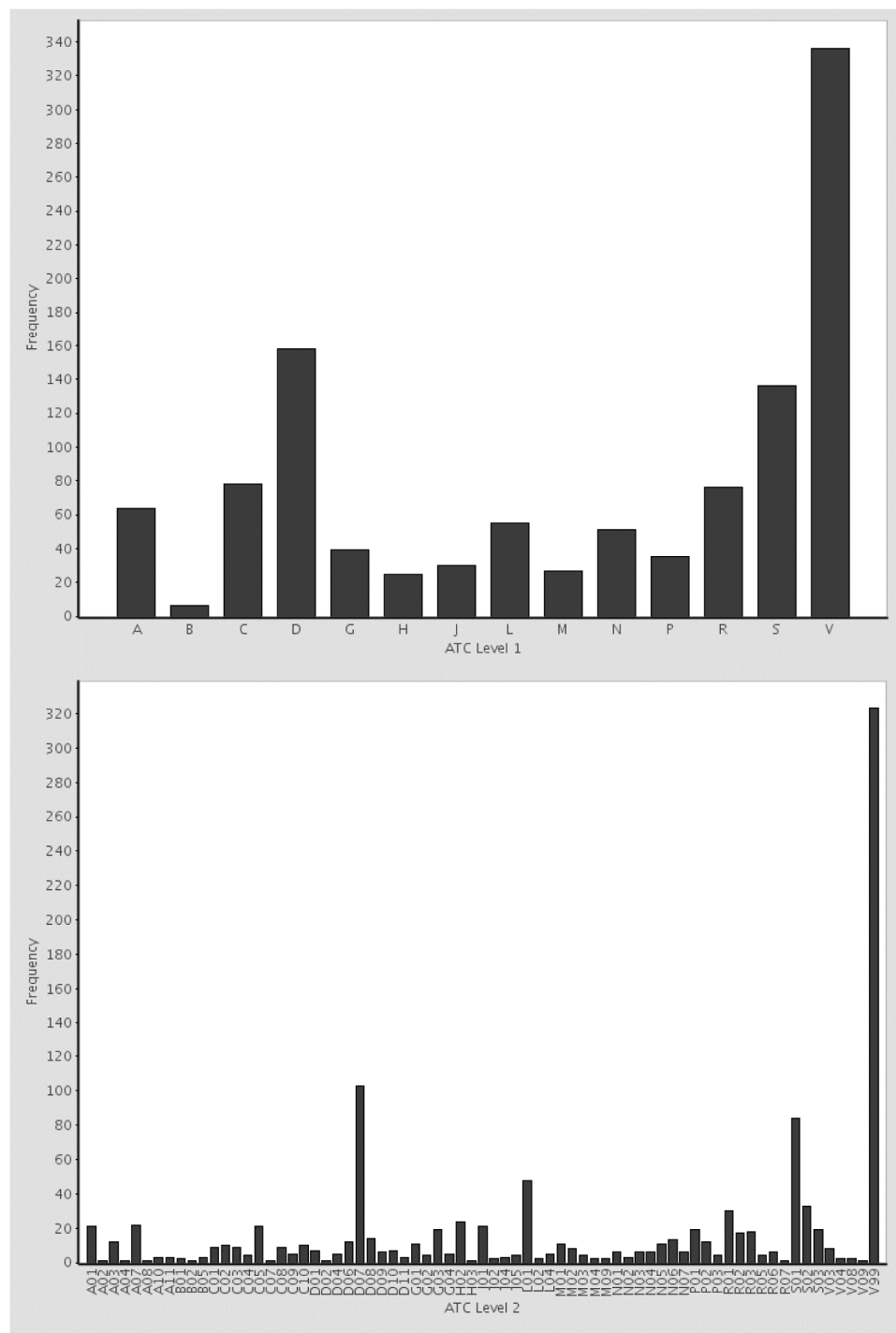
**Supplementary Figure S8: Quality control for primary screen of 5600 agents against  $\text{BCR-ABL}^{\text{T315I}}$  LICs performed in the presence of 0.85 ng/mL IL7. (a)** Distribution of  $\text{EC}_{50}$  of non-BCR-ABL-inhibiting reference compound staurosporine (calculated from wells 2A-2J in (d)). **(b)** Scatterplot of percent activity of the test compounds relative to controls. Good separation is seen between negative controls (red, DMSO-treated, max signal, column 13 in (d)) and positive controls (green, 300 nM staurosporine, min signal, column 14 in (d)). Test compounds showing statistically significant activity relative to background noise (negative controls, red) are depicted in blue; inactive test compounds are black. **(c)** Distribution of  $Z'$  values for each plate in the primary screen. All  $Z'$  values throughout the run – average=0.85, lowest=0.77, and highest=0.92 **(d)** Heat map comparison of well activity averaged across all plates. Wells 1A-1J and 2A-2J show serial dilutions of dasatinib and staurosporine tested against  $\text{BCR-ABL}^{\text{T315I}}$  LICs. Although 100 nM dasatinib (Well 1A) was totally ineffective, well 2A with highest staurosporine concentration (300 nM) showed average LIC growth inhibition of approximately 100%.



**Supplementary Figure S9: Primary high-throughput drug screening experiments capture BCR-ABL-KI drug-resistant phenotypes with high accuracy. Distributions of independent dose response curves of dasatinib and staurosporine against BCR-ABL<sup>WT</sup> and BCR-ABL<sup>T315I</sup> LICs in the presence of 0.85 ng/mL IL7 calculated separately from all assay plates (wells 1A-1J and 2A-2J) of primary drug screening experiments (also see Supplementary Fig. S7d and S8d) are presented. Both IL7-imparted dasatinib-resistant phenotype in BCR-ABL<sup>WT</sup> LICs (EC<sub>50</sub> in nM: 95%CI = 86-116, average >100) and BCR-ABL-mutation-imparted BCR-ABL-KI-resistant phenotype in BCR-ABL<sup>T315I</sup> LICs, similar to Figure 1b, were consistently captured across all plates. Low interplate variability in calculated EC<sub>50</sub> values was observed for the non-BCR-ABL-targeting reference compound staurosporine (95%CI for EC<sub>50</sub> in nM: WT = 11-12, T315I = 15-16) and majority of the validated hits (refer the Excel Supplement).**



**Supplementary Figure S10: Receiver Operating Characteristic (ROC) analysis demonstrates that both (a)  $BCR-ABL^{WT}$  and (b)  $BCR-ABL^{T315I}$  LIC-based assays have high discriminatory power (AUC 0.83 and 0.85, respectively). The ROC curve is plotted as a function of % activity, and is color coded according to the right Y-axis. The ROC curves in gray are calculated from 200 bootstrap simulations. The dashed line corresponds to a random assay.**



**Supplementary Figure S11: Frequency of ATC Level 1 (top) and ATC Level 2 (bottom) compounds for the 706 compounds submitted to secondary analysis.**

**Supplementary Table 1: Steps in optimized high-throughput screening assay (CTG readout)**

Step	Parameter	Value	Description
1	Plate cells	25 µL	Plate LICs $5 \times 10^4$ per mL (25 µL/well) in BCM10 + 0.85 ng/mL IL7 into 384-well opaque bottom white microplates using Wellmate (Matrix)
2	Primary drug screening controls in columns 1-2 and 13-14	25 nL	1A-1I: Nine dasatinib concentrations (100 nM, 30 nM, 10nM, 3 nM, 1 nM, 0.3 nM, 0.1 nM, 0.03 nM and 0.01 nM) – control for IL7- and BCR-ABL mutation-imparted resistance against BCR-ABL-KIs  2A-2I: Nine staurosporine concentrations (300 nM, 100 nM, 60 nM, 30 nM, 10 nM, 6 nM, 3 nM, 1 nM, 0.6 nM) – non-BCR-ABL-specific reference control in the presence of IL7  13A-13P, 1J, 2J: DMSO 0.1% ( <u>Max Signal OR Negative Control</u> ); 14A-14P: staurosporine at 300 nM ( <u>Min Signal OR Positive Control</u> ); 1K-1P, 2K-2P: 40 µM dasatinib  21A-21P: DMSO 0.1% ( <u>Max Signal</u> ); 22A-22P, 23K-24P, 24K-24P: staurosporine at 300 nM ( <u>Min Signal</u> )  23A-23J: Staurosporine – 10 log-fold dilutions (3 µM to 0.3 pM) - non-BCR-ABL-specific reference control in the presence of IL7  24A-24J: Dasatinib – 10 log-fold dilutions (1 µM to 0.1 pM) – control for IL7- and BCR-ABL mutation-imparted BCR-ABL-KI drug-resistance
2	Secondary drug screening controls in columns 21-24	25 nL	
3	Add <u>test</u> compounds in columns 3-12 and 15-24 in primary; columns 1-20 in secondary screen	25 nL	<u>Primary screening:</u> Single final drug concentration of 10 µM  <u>Secondary screening:</u> Triplicate ten half-log serial dilutions (5 µM to 2 nM final concentration) of primary screening hits to determine their half-maximal inhibitory concentrations (IC <sub>50</sub> ) against LICs  384-well master drug-stock plates prepared at 1000X in DMSO. Drug delivered to assay plates by pin transfer (using V&P Scientific pin tool, 10H pins), giving a final drug concentration of 1× and 0.1% DMSO in all control and test wells of assay plates
4	Incubation 1	72 h	Liconics incubator, 8%CO <sub>2</sub> , 37°C (standard LIC culture conditions)
5	Incubation 2	20 min	Room temp, low light (instructions as per Promega)
6	Add reagent	25 µL	CellTiter Glo (Promega) pre-equilibrated to RT before use
7	Incubation 3	25 min	Room temp, low light (per Promega)
8	Assay readout	ATP levels	Envision, Luminescent mode – ATP levels as a measure of LIC number and viable growth in 72 h – <u>Signal</u> measured in RLU
9	Data processing	Pipeline Pilot	% inhibition by test compound = $100 * (\text{Log}_{10}\text{Test Signal} - \text{Log}_{10}\text{Min Signal mean}) / (\text{Log}_{10}\text{Min Signal mean} - \text{Log}_{10}\text{Max Signal mean})$ Z-prime (Z') = $1 - [(3 * \text{stdev of Log}_{10}\text{Max Signal} + 3 * \text{stdev of Log}_{10}\text{Min Signal}) / (\text{Log}_{10}\text{Max Signal mean} - \text{Log}_{10}\text{Min Signal mean})]$ Z' is a dimensionless calculation

			to assess assay quality - for a good assay $Z \geq 0.5$ , and for a perfect assay $Z = 1$
--	--	--	---

## **Supplementary References**

1. Kocisko DA, Baron GS, Rubenstein R, Chen J, Kuizon S, Caughey B. New inhibitors of scrapie-associated prion protein formation in a library of 2000 drugs and natural products. *J Virol* 2003;77(19):10288-94.
2. Weissmann C, Aguzzi A. Approaches to therapy of prion diseases. *Annu Rev Med* 2005;56:321-44.
3. Team RDC. R: A language and environment for statistical computing. Vienna, Austria: R Foundation for Statistical Computing; 2009.
4. Ritz C, Streibig JC. Bioassay Analysis using R. *J Statist Software* 2005;12 (5)(5):22.
5. Sing T, Sander O, Beerenwinkel N, Lengauer T. ROCR: visualizing classifier performance in R. *Bioinformatics* 2005;21(20):3940-1.
6. Smoot ME, Ono K, Ruscheinski J, Wang PL, Ideker T. Cytoscape 2.8: new features for data integration and network visualization. *Bioinformatics* 2011;27(3):431-2.
7. Snead JL, O'Hare T, Adrian LT, *et al.* Acute dasatinib exposure commits Bcr-Abl-dependent cells to apoptosis. *Blood* 2009;114(16):3459-63.
8. Luo FR, Yang Z, Camuso A, *et al.* Dasatinib (BMS-354825) pharmacokinetics and pharmacodynamic biomarkers in animal models predict optimal clinical exposure. *Clin Cancer Res* 2006;12(23):7180-6.

Worksheet	Description	Legend	Notes
Host Factors	The effect of 15 leukemia-microenvironment relevant cytokines on dasatinib potency ( $EC_{50}$ ) against Arf-/BCR-ABLWT LICs	<ul style="list-style-type: none"> <li>* <b>hostFactor</b>: cytokine name</li> <li>* <b>conc</b>: cytokine concentration</li> <li>* <b>hill</b>: hill slope</li> <li>* <b>EC<sub>50</sub></b>: dasatinib EC<sub>50</sub> (nM)</li> <li>* <b>EC<sub>50</sub>CI</b>: EC<sub>50</sub> 95% confidence interval</li> <li>* <b>r<sup>2</sup></b>: r-squared of the non-linear regression</li> <li>* <b>sample</b>: St. Jude registration number (regnumber + batch number)</li> <li>* <b>regnumber</b>: St. Jude registration root number</li> <li>* <b>supplier name</b>: name of the chemical supplier for this compounds</li> <li>* <b>supplier ID</b>: vendor unique identifier</li> <li>* <b>salt name</b>: name of any salt present</li> <li>* <b>salt eqs.</b>: number of salt equivalents</li> <li>* <b>solvate name</b>: name of any solvate present</li> <li>* <b>solvate eqs.</b>: number of solvate equivalents</li> <li>* <b>formula weight</b>: total molecular weight of all species present in the sample</li> <li>* <b>molsmiles</b>: molecular SMILES</li> <li>* <b>synonym</b>: alternate names for this compound</li> <li>* <b>Name of clinical anti-leukemic agent</b></li> <li><b>WT_EC<sub>50</sub></b>: mouse wild-type BCR-ABL B-cell EC<sub>50</sub> (μM)</li> <li>* <b>WT_EC<sub>50</sub>CI</b>: WT EC<sub>50</sub> 95% confidence interval</li> <li>* <b>WT_actclass</b>: WT activity classification</li> <li>* <b>WT_curveScore</b>: grade for quality of the WT dose-response curve (see Supplemental for details)</li> <li>* <b>T315I_EC<sub>50</sub></b>: mouse T315I BCR-ABL B-cell EC<sub>50</sub> (μM)</li> <li>* <b>T315I_EC50CI</b>: T315I EC50 95% confidence interval</li> <li>* <b>T315I_actclass</b>: T315I activity classification</li> <li>* <b>T315I_curveScore</b>: grade for quality of the T315I dose-response curve (see Supplemental for details)</li> </ul>	Triplicate measurements were pooled and fit to a single curve using a two parameter logistic model (bottom fixed to 0% and top fixed to 100%)
Structure	Structural information for 706 compounds	<ul style="list-style-type: none"> <li>* <b>WT_EC<sub>50</sub></b>: mouse wild-type BCR-ABL B-cell EC<sub>50</sub> (μM)</li> <li>* <b>WT_EC<sub>50</sub>CI</b>: WT EC<sub>50</sub> 95% confidence interval</li> <li>* <b>WT_actclass</b>: WT activity classification</li> <li>* <b>WT_curveScore</b>: grade for quality of the WT dose-response curve (see Supplemental for details)</li> <li>* <b>T315I_EC<sub>50</sub></b>: mouse T315I BCR-ABL B-cell EC<sub>50</sub> (μM)</li> <li>* <b>T315I_EC50CI</b>: T315I EC50 95% confidence interval</li> <li>* <b>T315I_actclass</b>: T315I activity classification</li> <li>* <b>T315I_curveScore</b>: grade for quality of the T315I dose-response curve (see Supplemental for details)</li> </ul>	
Screen Summary (1)	List of 15 clinically-used conventional anti-leukemic agents validated during dose-response screening experiments	<ul style="list-style-type: none"> <li>* <b>WT_EC<sub>50</sub></b>: mouse wild-type BCR-ABL B-cell EC<sub>50</sub> (μM)</li> <li>* <b>WT_EC<sub>50</sub>CI</b>: WT EC<sub>50</sub> 95% confidence interval</li> <li>* <b>WT_actclass</b>: WT activity classification</li> <li>* <b>WT_curveScore</b>: grade for quality of the WT dose-response curve (see Supplemental for details)</li> <li>* <b>T315I_EC<sub>50</sub></b>: mouse T315I BCR-ABL B-cell EC<sub>50</sub> (μM)</li> <li>* <b>T315I_EC50CI</b>: T315I EC50 95% confidence interval</li> <li>* <b>T315I_actclass</b>: T315I activity classification</li> <li>* <b>T315I_curveScore</b>: grade for quality of the T315I dose-response curve (see Supplemental for details)</li> </ul>	Conventional anti-leukemic agents - Cladribine, Clofarabine, Decitabine, Fludarabine, Nelarabine and Pentostatin, all of which are nucleoside analogs/antimetabolites, were originally not present among agents tested; many agents with similar MOA were validated. Other clinical anti-leukemic agents which belong to categories - antibody, growth factors, enzymes or oligonucleotides, are not compatible to HTS and were not present in the tested compound library.
Screen Summary (2)	Complete dose-response screening data for 706 compounds	<ul style="list-style-type: none"> <li>* <b>WT_EC<sub>50</sub></b>: mouse wild-type BCR-ABL B-cell EC<sub>50</sub> (μM)</li> <li>* <b>WT_EC<sub>50</sub>CI</b>: WT EC<sub>50</sub> 95% confidence interval</li> <li>* <b>WT_actclass</b>: WT activity classification</li> <li>* <b>WT_curveScore</b>: grade for quality of the WT dose-response curve (see Supplemental for details)</li> <li>* <b>T315I_EC<sub>50</sub></b>: mouse T315I BCR-ABL B-cell EC<sub>50</sub> (μM)</li> <li>* <b>T315I_EC50CI</b>: T315I EC50 95% confidence interval</li> <li>* <b>T315I_actclass</b>: T315I activity classification</li> <li>* <b>T315I_curveScore</b>: grade for quality of the T315I dose-response curve (see Supplemental for details)</li> <li>* <b>comment</b>: comments on - observed differential activity</li> </ul>	A few compounds showed differential activity between WT and T315I. Most of these are annotated with "Differential activity within experimental error", indicating that there was sufficient uncertainty in the curve fit or that the differences are a result of the hard cutoffs applied for activity classification and are not significant.

ATC Classification

ATC classification for 706 compounds

- \* **ATC\_L1:** Anatomical Therapeutic Chemical (ATC) Classification System first level  
(anatomical main group)
- \* **ATC\_L2:** Anatomical Therapeutic Chemical (ATC) Classification System second level  
(therapeutic main group)
- \* **ATC\_L3:** Anatomical Therapeutic Chemical (ATC) Classification System third level  
(therapeutic/pharmacological subgroup)
- \* **ATC\_L4:** Anatomical Therapeutic Chemical (ATC) Classification System fourth level  
(chemical/therapeutic/pharmacological subgroup)

hostFactor	conc	hill	EC <sub>50</sub>	EC <sub>50</sub> CI	r <sup>2</sup>
IL3	0.0 ng/ml	0.5391	5.1118	3.8724 - 6.7479	0.987
IL3	0.01 ng/mL	0.4619	7.5159	5.4628 - 10.3405	0.983
IL3	0.1 ng/mL	0.3164	22.1664	12.1764 - 40.3525	0.944
IL3	1 ng/mL	0.3553	23.3197	14.1087 - 38.5443	0.958
IL3	10 ng/mL	0.3911	22.5621	14.9315 - 34.0924	0.971
IL3	100 ng/mL	0.4276	21.5773	15.2841 - 30.4619	0.979
IL15	0.0 ng/ml	0.5374	4.5252	3.4241 - 5.9805	0.987
IL15	0.01 ng/mL	0.5456	4.7956	3.6317 - 6.3325	0.987
IL15	0.1 ng/mL	0.5223	5.1369	3.9508 - 6.6792	0.988
IL15	1 ng/mL	0.5639	4.6853	3.4341 - 6.3924	0.984
IL15	10 ng/mL	0.5474	4.8593	3.7109 - 6.3630	0.987
IL15	100 ng/mL	0.5803	4.2075	3.2656 - 5.4211	0.989
IL6	0.0 ng/ml	0.5269	4.5635	3.2798 - 6.3497	0.982
IL6	0.01 ng/mL	0.5395	4.6483	3.4190 - 6.3197	0.984
IL6	0.1 ng/mL	0.5771	4.2131	3.1209 - 5.6876	0.984
IL6	1 ng/mL	0.5312	4.645	3.4403 - 6.2716	0.984
IL6	10 ng/mL	0.5605	4.494	3.4060 - 5.9295	0.986
IL6	100 ng/mL	0.5772	4.4834	3.4583 - 5.8123	0.988
SCF	0.0 ng/ml	0.5433	5.0496	3.8776 - 6.5759	0.988
SCF	0.01 ng/mL	0.5206	5.1184	3.7436 - 6.9982	0.984
SCF	0.1 ng/mL	0.5289	4.7638	3.5384 - 6.4137	0.985
SCF	1 ng/mL	0.5263	4.9426	3.7637 - 6.4909	0.987
SCF	10 ng/mL	0.5293	4.9611	3.5256 - 6.9812	0.98
SCF	100 ng/mL	0.5473	4.8079	3.7504 - 6.1636	0.989
FLT3	0.0 ng/ml	0.5785	4.0982	2.9655 - 5.6635	0.982
FLT3	0.01 ng/mL	0.5549	3.251	2.3904 - 4.4215	0.984
FLT3	0.1 ng/mL	0.5837	4.0456	3.1306 - 5.2282	0.988
FLT3	1 ng/mL	0.5677	4.1235	2.9621 - 5.7402	0.981
FLT3	10 ng/mL	0.567	3.6648	2.7944 - 4.8065	0.987
FLT3	100 ng/mL	0.6116	3.9157	2.9477 - 5.2015	0.986
IL4	0.0 ng/ml	0.494	6.2811	4.3841 - 8.9990	0.979
IL4	0.01 ng/mL	0.4721	7.6786	5.1536 - 11.4406	0.974
IL4	0.1 ng/mL	0.4582	10.607	7.3974 - 15.2093	0.978
IL4	1 ng/mL	0.4529	11.2471	7.8367 - 16.1418	0.978
IL4	10 ng/mL	0.4687	10.4343	7.1849 - 15.1533	0.977
IL4	100 ng/mL	0.4579	11.1402	7.6311 - 16.2629	0.976
TSLP	0.0 ng/ml	0.5017	4.9482	3.5263 - 6.9434	0.981
TSLP	0.01 ng/mL	0.4805	5.692	3.8453 - 8.4256	0.975
TSLP	0.1 ng/mL	0.5043	8.314	6.0702 - 11.3872	0.983
TSLP	1 ng/mL	0.456	13.35	10.1901 - 17.4896	0.987
TSLP	10 ng/mL	0.4007	18.4296	12.8535 - 26.4247	0.978
TSLP	100 ng/mL	0.4177	17.6412	11.9235 - 26.1008	0.974
MCSF	0.0 ng/ml	0.5307	4.8682	3.5748 - 6.6296	0.984
MCSF	0.01 ng/mL	0.5375	4.803	3.0670 - 7.5216	0.968
MCSF	0.1 ng/mL	0.5247	5.4838	3.8284 - 7.8550	0.979
MCSF	1 ng/mL	0.5357	4.6983	3.2180 - 6.8595	0.977
MCSF	10 ng/mL	0.517	4.6896	3.2354 - 6.7975	0.978
MCSF	100 ng/mL	0.5489	4.943	3.4050 - 7.1756	0.978
IL9	0.0 ng/ml	0.5582	4.2149	2.9368 - 6.0491	0.979
IL9	0.01 ng/mL	0.5585	4.3679	3.0111 - 6.3359	0.977
IL9	0.1 ng/mL	0.5698	4.0533	2.8653 - 5.7341	0.98
IL9	1 ng/mL	0.538	4.6609	3.1394 - 6.9198	0.975
IL9	10 ng/mL	0.5789	4.4575	2.8883 - 6.8792	0.97
IL9	100 ng/mL	0.5306	5.3572	3.5917 - 7.9905	0.975
GMCSF	0.0 ng/ml	0.4922	4.9682	3.4753 - 7.1024	0.979
GMCSF	0.01 ng/mL	0.5195	4.4331	3.1515 - 6.2359	0.981
GMCSF	0.1 ng/mL	0.4903	5.2002	3.7301 - 7.2496	0.982
GMCSF	1 ng/mL	0.5287	5.0754	3.5354 - 7.2862	0.978
GMCSF	10 ng/mL	0.4985	5.1825	3.6136 - 7.4324	0.979
GMCSF	100 ng/mL	0.5077	5.2664	3.9156 - 7.0832	0.985
CXCL12	0.0 ng/ml	0.5302	4.2517	3.0049 - 6.0157	0.98
CXCL12	0.01 ng/mL	0.5506	4.02	2.8966 - 5.5790	0.982
CXCL12	0.1 ng/mL	0.555	4.3428	3.0724 - 6.1384	0.98
CXCL12	1 ng/mL	0.5543	4.9481	3.5552 - 6.8868	0.982
CXCL12	10 ng/mL	0.5257	6.341	4.6141 - 8.7143	0.983
CXCL12	100 ng/mL	0.5626	7.7776	5.4588 - 11.0814	0.979
GCSF	0.0 ng/ml	0.4859	5.3848	3.8070 - 7.6163	0.98
GCSF	0.01 ng/mL	0.4888	5.6829	4.1379 - 7.8048	0.983
GCSF	0.1 ng/mL	0.4995	5.2436	3.5467 - 7.7522	0.975
GCSF	1 ng/mL	0.5238	4.4557	2.9858 - 6.6491	0.974
GCSF	10 ng/mL	0.5082	5.5333	3.8070 - 8.0422	0.977
GCSF	100 ng/mL	0.5071	5.5916	3.8599 - 8.1003	0.978
TGFb	0.0 ng/ml	0.5196	4.4138	3.1588 - 6.1674	0.981
TGFb	0.01 ng/mL	0.8345	2.0792	1.3877 - 3.1152	0.972
TGFb	0.1 ng/mL	1.3386	1.0712	0.6824 - 1.6815	0.943
TGFb	1 ng/mL	1.1768	1.2921	0.8022 - 2.0810	0.949
TGFb	10 ng/mL	1.0645	1.4597	0.8969 - 2.3756	0.954
TGFb	100 ng/mL	1.258	1.4057	0.8535 - 2.3151	0.947
IL2	0.0 ng/ml	0.5186	4.3969	3.0447 - 6.3495	0.978
IL2	0.01 ng/mL	0.4837	4.8218	3.3902 - 6.8578	0.98

IL2	0.1 ng/mL	0.4856	4.531	3.0037 - 6.8346	0.974
IL2	1 ng/mL	0.51	4.4851	3.1998 - 6.2866	0.981
IL2	10 ng/mL	0.5181	4.753	3.2444 - 6.9630	0.977
IL2	100 ng/mL	0.507	4.6062	3.3039 - 6.4219	0.982
IL7	0.0 ng/ml	0.4659	7.0902	5.2763 - 9.5276	0.985
IL7	0.01 ng/mL	0.3318	61.9094	41.1312 - 93.1840	0.971
IL7	0.1 ng/mL	0.3661	251.4246	157.6730 - 400.9203	0.958
IL7	1 ng/mL	0.3761	281.2124	165.0664 - 479.0824	0.947
IL7	10 ng/mL	0.383	286.5185	173.4620 - 473.2615	0.95
IL7	100 ng/mL	0.352	448.189	245.0635 - 819.6787	0.938



Name of clinical anti-leukemic agent	sample	WT_EC <sub>50</sub>	WT_EC <sub>50</sub> CI	WT_curveScore	WT_actclass	T315L_EC <sub>50</sub>	T315L_EC <sub>50</sub> CI	T315L_curveScore	T315L_actclass
CYTARABINE	SJ000285188-6	0.0639	0.0425 - 0.0961	A113	HIGH	0.0603	0.0355 - 0.1023	A113	HIGH
MELPHALAN*	SJ000285194-4	>5	NA	C555	WEAK	3.9408	NA	C555	WEAK
MERCAPTOPURINE	SJ000285195-2	0.0211	0.0013 - 0.3518	A111	HIGH	0.0444	0.0342 - 0.0575	B110	HIGH
METHOTREXATE	SJ000285196-2	0.0225	0.0014 - 0.3699	A111	HIGH	0.0438	0.0316 - 0.0606	A112	HIGH
THIOGUANINE	SJ000285208-3	0.0441	0.0248 - 0.0786	B110	HIGH	0.0202	0.0010 - 0.4084	B110	HIGH
AMINOPTERINE	SJ000285221-4	<0.1	NA	B110	HIGH	<0.1	NA	B110	HIGH
AZACITIDINE	SJ000285227-1	1.2936	0.9338 - 1.7920	B311	WEAK	1.2871	0.8082 - 2.0498	B311	WEAK
ETOPOSIDE	SJ000285235-3	0.1369	0.1148 - 0.1632	A212	MED	0.1368	0.1164 - 0.1608	A212	MED
MITOXANTRONE	SJ000285321-4	0.0433	0.0348 - 0.0539	A112	HIGH	0.044	0.0361 - 0.0536	A112	HIGH
HYDROCORTISONE	SJ000285358-5	0.1905	0.1782 - 0.2036	A212	MED	0.19	0.1788 - 0.2020	A212	MED
PREDNISOLONE	SJ000285541-3	0.1573	0.1495 - 0.1654	A212	MED	0.1541	0.1406 - 0.1689	A212	MED
DEXAMETHASONE	SJ000285729-2	<0.1	0.0039 - 4.1318	B110	HIGH	0.0374	0.0102 - 0.1371	B110	HIGH
AMSACRINE	SJ000285974-2	0.0861	0.0767 - 0.0967	A112	HIGH	0.0747	0.0627 - 0.0889	A112	HIGH
IDARUBICIN	SJ000287925-2	<0.1	NA	B110	HIGH	<0.1	NA	B110	HIGH
VINCRISTINE	SJ000288244-2	0.1045	0.0914 - 0.1194	A213	MED	0.1311	0.0021 - 8.2851	A214	MED

\*often performs poorly in HTS











SJ000288274-2	>5	NA	D555	INACTIVE	>5	NA	D555	INACTIVE
SJ000288278-2	0.0149	0.0104 - 0.0214	B110	HIGH	0.0159	0.0113 - 0.0225	B110	HIGH
SJ000288284-2	>5	NA	D555	INACTIVE	>5	NA	C555	INACTIVE
SJ000288304-1	>5	NA	C555	INACTIVE	>5	NA	C555	INACTIVE
SJ000288306-1	0.306	0.1694 - 0.5530	A211	MED	0.171	0.0776 - 0.3768	A211	MED
SJ000288308-1	>5	NA	B341	INACTIVE	>5	NA	B344	INACTIVE
SJ000288312-1	>5	NA	D555	INACTIVE	>5	NA	C555	INACTIVE
SJ000288313-1	>5	NA	D555	INACTIVE	>5	NA	D555	INACTIVE
SJ000288316-1	>5	NA	C555	INACTIVE	>5	NA	C555	INACTIVE
SJ000288318-1	>5	NA	D555	INACTIVE	>5	NA	D555	INACTIVE
SJ000288320-1	>5	NA	C555	INACTIVE	>5	NA	C555	INACTIVE
SJ000288325-1	>5	NA	B333	INACTIVE	4.198	4.0769 - 4.3227	B313	WEAK
SJ000288326-1	>5	NA	A241	INACTIVE	>5	NA	B341	INACTIVE
SJ000288327-1	>5	NA	D555	INACTIVE	>5	NA	D555	INACTIVE
SJ000288328-1	>5	NA	C555	INACTIVE	>5	NA	C555	INACTIVE
SJ000518967-1	0.3177	0.2999-0.3357	A212	MED	0.3133	0.2964-0.3311	A212	MED
SJ000518972-1	0.3581	0.3459-0.3639	A212	MED	0.3311	0.3206-0.3428	A212	MED

Differential activity within experimental error

DIHYDROARTEMISININ  
ARTESUNATE

